Princeton University

Branching Morphogenesis and Epithelial Fusion in Embryonic Development of Avian Lungs

Author:
Dror Liebenthal

Supervisor:
Professor Celeste Nelson

Submitted in partial fulfillment of the requirements
for the degree of Bachelor of Science in Engineering

in the

Department of Chemical and Biological Engineering
and Engineering Biology Certificate

April 2015

Declaration of Authorship

This paper represents my own work in accordance with University regulations

I authorize Princeton University to lend this thesis to other institutions or individuals for the purpose of scholarly research.

Signature: _____

Name: _____

I further authorize Princeton University to reproduce this thesis by photocopying or by other means, in total or in part, at the request of other institutions or individuals for the purpose of scholarly research.

Signature: _____

Name: _____

Princeton University requires the signatures of all persons using or photocopying this thesis. Please sign below, and give address and date.

Name:	*Address:*	*Date:*

Acknowledgements

I'd like to first thank Professor Nelson for the amazing feedback and guidance she has given me throughout this process. I first decided I'd like to work with her after taking her class on the Physical Basis of Human Disease in the spring of my junior year, and I could not be more happy with the way it has turned out. From when I first joined her lab in the summer until now, she has been an outstanding thesis advisor every step of the way, both making sure that I stayed on track and giving me the leeway to take this thesis in the directions that I wanted.

This thesis would also not have been possible without all the members of the Nelson Group. In particular, I'd like to thank Victor Varner and Mei Fong Pang for taking the time to help me with the experimental procedures. I'd also like to thank Siu-Yuan Huang, an alumnus of the lab whose past research served as the basis for my work, and who provided me with valuable guidance in the early stages of my research.

An enormous thank you is also due to the fantastic friends I've had over the course of my four years here, be they from TI, Chipper, or elsewhere. Getting to know you all has been the single greatest pleasure of my Princeton experience, and I look forward to seeing all you accomplish in the future.

I'd also like to especially thank Michael Wiest and Lindsey Bergh, without whom I cannot begin to imagine what my experience in the Chemical and Biological Engineering Department would've been like. With your company, we somehow managed to turn the endless problem sets, exams, and projects over the last few years into good memories, and have kept each other sane in the process.

Finally, I'd like to dedicate this thesis to my family. To Mom, Dad, Nir, and Oren: whenever I stop to think about the path my life has taken, I'm always amazed by how unpredictable, unique, and fulfilling it has been throughout. A lot has changed since we first left Israel when I was four, but you have been the one constant. I love all of you and always will. I hope to never lose my appreciation for the support and love you've given me, and the love of adventure and sense of wonder you've instilled in me. It's always been us.

Abstract

Little is known about the program of branching morphogenesis in embryonic chicken lungs, particularly with regards to the role that various molecules in the lung environment might play in directing branching, growth, and fusion. A better understanding of how branching morphogenesis is controlled is extremely important to the field of lung tissue engineering, which is a possible future way to improve the standard of treatment for lung diseases. Characterization of the program of development of chicken lungs also has important evolutionary implications, as avian lungs differ drastically from mammalian lungs, featuring several differences that enable far greater gas exchange efficiency in birds. This study characterizes the program of branching, growth, and fusion via an immunostaining and epifluorescent imaging approach, achieving a large improvement in image quality over any previous work exploring lung development in chickens. In particular, the study focuses on an area at which opposing sets of parabronchi approach each other, interweave, and exhibit profuse anastomosis at Day 11-12 of development. This growth is quantified and supports the possibility that a reaction-diffusion model may be a potential control mechanism for growth and fusion in this lung geometry. Furthermore, the study assesses the usefulness of two candidate open window procedures for the sake of providing a viable way to manipulate molecules in the lung environment *in ovo* to understand their function. Initial results from one of them, the Minimal Invasion procedure, suggest that it may be an effective way to successfully elucidate the role of a variety of molecules associated with epithelial growth. Finally, immunostains for β-catenin, DAPI, vimentin, and Slug are carried out, and Slug is identified as a target molecule for manipulation in future open window trials due to its pattern of higher concentration between opposing parabronchi directly prior to fusion.

Contents

List of Figures

List of Tables

Abbreviations

BMP	**B**one **M**orphogenetic **P**rotein
COPD	**C**hronic **O**bstructive **P**ulmonary **D**isease
DAPI	4' 6-**dia**mino-2-**p**henylindole d**i**hydrochloride
FGF	**F**ibroblast **G**rowth **F**actor
HH(XX)	**H**amburger **H**amilton Day **XX**
MA	**M**aximal **A**ccess
MI	**M**inimal **I**nvasion
PBS	**P**hosphate **B**uffered **S**aline
ROA	**R**idge **O**f **A**nastomosis
SHH	**S**onic **H**edge**H**og
TGF	**T**ransforming **G**rowth **F**actor

Background

Motivation

In 2012, chronic obstructive pulmonary disease (COPD) was the cause of over 3 million deaths across the world, over 90% of which occurred in lower to middle income countries [47]. In the US, COPD was the third leading cause of death in 2011, with 15 million Americans having reported diagnosis. Additionally, approximately 50% of adults deal with low pulmonary functionality, without being aware that they have COPD [7]. Although this disease is widely prevalent and a large cause of death throughout the world, effective treatment options for COPD and other lung diseases are severely lacking.

As human lung tissue does not have the capacity to regenerate or repair itself beyond a microscopic level, the current primary solution for severely damaged lungs is a lung transplantation procedure. However, this expensive procedure is limited by a large shortage in organ donors, and has only been demonstrated to achieve 10-20% survival at 10 years after the procedure [33]. Complications with the procedure are significant, including primary graft dysfunction, infection, and *bronchiolitis obliterans* syndrome, and it is unclear whether the transplant even confers a survival advantage to the patient [22].

Even in non-fatal cases, lung disease has a large negative impact on quality of life, as problematic respiratory complaints, fear, social isolation, anxiety, depression, dyspnea, hypoxemia, and more are commonly seen in patients. The lack of treatment options and decline in quality of life is so severe in advanced lung disease

that the accepted practice is to shift focus to end of life care rather than curative treatment [12].

Recent progress in the field of lung tissue engineering suggests that this approach may be a possible replacement for lung transplantation as the primary treatment for COPD and other severe lung diseases [5]. However, lung development in humans features highly stereotyped branching morphogenesis, the program by which the complex structural framework of the lung forms, including development of the bronchi and bronchioles. It is currently a topic of debate whether the regulatory processes governing this development are bound by a common principle across organisms, and to what extent geometrical and physical constraints play a role [18]. An improved understanding of branching morphogenesis in humans will be extremely advantageous to the progress of lung tissue engineering, and may begin to be approached by first understanding branching morphogenesis in other lung systems, like birds.

As additional motivation, the study of branching morphogenesis in chicken lungs has evolutionary implications as well, as mammals and birds have evolved drastically different lungs. In mammals, bronchioles, alveolar ducts, and alveoli are responsible for both ventilation and gas exchange. Less than 20% of the lung by volume functions to ventilate the airways. In contrast, avian lungs make use of air sacs to separate ventilation and gas exchange functions [27, 34]. Avian parabronchi, the smaller epithelial projections arising from avian bronchi, are parallel and exhibit profuse anastomosis during embryonic development [23]. They are perfused perpendicularly by pulmonary blood vessels, indicating that gas exchange in avian lungs can be modeled as a cross-current exchange system [27, 34]. This results in a greater efficiency of gas exchange in birds compared to mammals, an adaptation that helps birds meet gas exchange needs at high altitudes [34]. The avian lung is 75% that of comparably sized mammals by volume, but provides 15% more surface area for gas exchange [26]. Studying the program of lung development and the associated lung environment molecules will thus contribute both to lung tissue engineering efforts and to our understanding of how the highly efficient lungs present in birds may have evolved.

1.1 Evolutionary Implications

The parabronchi in avian lungs allow for unidirectional airflow during both inspiration and expiration. In mammals, airflow is tidal, and the terminal alveoli act as cul-de-sacs, reducing the efficiency of gas exchange compared to birds. Airflow has been determined to be unidirectional in regions of the lungs of alligators as well. Alligator lungs lack air sacs, but do exhibit an aerodynamic valve analogous to that seen in the avian lung. Dorsal bronchi are connected in the alligator lung through a large number of anastomosed parabronchi, but it is not clear how unidirectional flow is achieved in alligators without the presence of air sacs and diaphragmatic breathing. Unidirectional flow is thought to have evolved prior to divergence of crurotarsan and dinosaurian archosaurs [10]. Further research has indicated that the branching angles in the arrangement of alligator primary and secondary bronchi seem to play a role in accomplishing unidirectional air flow during both inspiration and expiration [38].

Unidirectional flow has also been reported in savannah monitor lizards [37], and recently, iguana lungs as well. Iguana lungs exhibit unidirectional air flow despite sharing little natural history with birds and lacking the anatomical features thought to be responsible for unidirectional air flow in birds, including parabronchi and air sacs. Unidirectional flow was previously thought to have developed in birds as a way of meeting gas exchange needs at high altitude, when oxygen is more scarce. However, these recent findings indicate that a new paradigm shift is necessary, and that the evolutionary driver of unidirectional flow may be different than previously thought. Additionally, this shows that unidirectional flow is possible in structurally simple lungs. However it is still possible that this phenomenon developed in iguanas due to convergent evolution. [8].

The respiratory system of *Drosophila melanogaster* is relevant as a paradigm of branching morphogenesis, and develops by sequentially branching into primary, secondary, and terminal branches. It is controlled by a program using FGF and FGF receptor (FGFR) repeatedly for branch budding and outgrowth. The pattern

of expression of the molecule and its receptor change at each stage of branching, resulting in new concentration gradients and different growth patterns [11]. Identification of the FGF family of molecules in fruit flies has been critical, as these morphogens have since been found to play a role in a large variety of lung systems, including those of mice and chicken [3, 20]. For example, treatment of explanted embryonic mouse epithelium with FGF10 has been shown to induce branching [3]. Further elucidation and comparison of the morphogen signaling systems present in mice, chicken, and reptiles will make the evolutionary history of air sacs and unidirectional air flow more clear.

1.2 Branching Morphogenesis in Chicken Lungs

Branching morphogenesis is a dynamic process in which epithelial cells either move within the tissue or extend and retract during branch formation and progression. Differential growth, cell invasion, epithelial folding, and matrix-driven branching are all mechanisms that may play a role [45]. The recursive branching responsible for transforming the developing lung from a simple tube to a complex system of airways is monopodial in the early chicken embryo and is controlled by a system of growth factors that is not fully understood. Apical constriction of epithelium in the lungs has been found to be a sufficient force in driving the cell and tissue changes necessary to implement initial monopodial budding. Apical constriction is driven by actomyosin contraction, and is a conserved morphogenetic mechanism. Moreover, patterned proliferation of the epithelium has been found to not be capable of fully accounting for the shape of newly formed buds, even in coordination with apical constriction, and may actually be entirely unnecessary for normal initiation of monopodial budding [20].

Although the signaling system responsible for directing branching morphogenesis is still unknown, Gleghorn *et al.* have created a 3D model of the chicken lung and used it to assess whether observed monopodial branching patterns can arise as a result of autocrine inhibition alone. They find that, at later stages, predicted

concentrations of a hypothetical inhibitory morphogen do not align with sites of branching, indicating that autocrine inhibition is not the main pathway responsible for control of branching. Additionally, morphometric analysis of positions of lung buds points to the determination of branching sites as being scaled in relation to the size of the organ. Finally an additional morphogen, transcription growth factor beta (TGFβ)1, is identified that is associated with rate of branch growth, but not specification of branch location [13]. Future research focusing on selective inhibition of molecules in the lung identified by Gleghorn *et al.*, such as sonic hedgehog (SHH), bone morphogenetic protein (BMP)4, and fibroblast growth factor (FGF)10 will allow for further elucidation of the control program of branching morphogenesis [13].

A possible way to model control of branching morphogenesis is through application of reaction-diffusion principles first proposed by Alan Turing, a phenomenon widely present across a variety of biological systems in which pattern formation events occur. By assuming initial homogenous morphogen (at least one activator and one inhibitor) distribution with slight perturbations, a linearity assumption can be made and general reaction rate functions can be replaced by linear ones. Reaction-diffusion models consist of partial differential equations describing spatial morphogen concentrations over time. The result is the formation of a wave pattern of morphogen concentrations with no time variation, aside from a gradual increase in amplitude [44]. For the case of the embryonic chicken lung, morphogens may be produced either by epithelial or mesenchymal cells, and may diffuse out of the cells with a well-defined rate of diffusion that is specified by the cell and molecule type.

A ligand-receptor reaction-diffusion model has successfully been developed for embryonic mouse lungs, in which FGF10 and SHH direct outgrowth of the lung bud. Menshykau *et al.* show that such a model can predict growth fields in the development of lung buds and might also account for the observed switches in domain branching, planar and orthogonal bifurcations, and trifurcations [31]. Adapting a ligand-receptor based Turing model for avian lungs would have to account for the widespread anastomosis events occurring throughout bird lung development.

This study will carry out preliminary exploration of the relevance of such reaction-diffusion systems to chicken lung geometry by characterizing the program of lung development via a series of immunostains targeting LCAM (a chicken homolog of E-cadherin, a cell adhesion protein present in epithelial tissue), β-catenin (an intracellular protein thought to be involved in EMT), and vimentin (an EMT marker intermediate filament protein expressed in mesenchymal cells). In particular, the distances between approaching parabronchi will be compared to distances over which morphogens in reaction-diffusion systems are thought to act.

1.3 Epithelial Fusion

On day 9 of embryonic development, numerous parabronchi radiate outwards from secondary bronchi in the avian lung. The parabronchi elongate into adjacent regions of mesenchymal cells before anastomosing profusely between Days 10 and 13, covering the surface of the lung and interconnecting the secondary bronchi [24]. As the two sets of parallel parabronchi approach at Day 11-12, the growing epithelial tips bifurcate, allowing parabronchial circuits to form by anastomosis of adjacent branches. A schematic of this process is shown in Figure 1.1 on the following page. Although the chicken parabronchi are hollow tubes lined with columnar epithelial cells and surrounded by mesenchymal tissue, this smooth cross-section begins to deteriorate as anastomosis begins. Outpouchings made of epithelial strands begin to develop from the epithelium and become canalized, allowing diverticula, or hollow outpouching structures, to arise from the central lumen [19]. The parabronchi increase in girth, and a network of air capillaries forms from atrial outpouchings. The epithelial cells of the air capillaries are squamous [28]. By Day 13, the basement membrane becomes conspicuous, with a thin barrier being formed by attenuation of epithelial cells as air capillaries invade the mesenchymal tissue [25].

The thin blood-air barrier is formed in mammalian lungs by conversion of alveolar type II cells to alveolar type I cells, or change from an alveolar caretaker

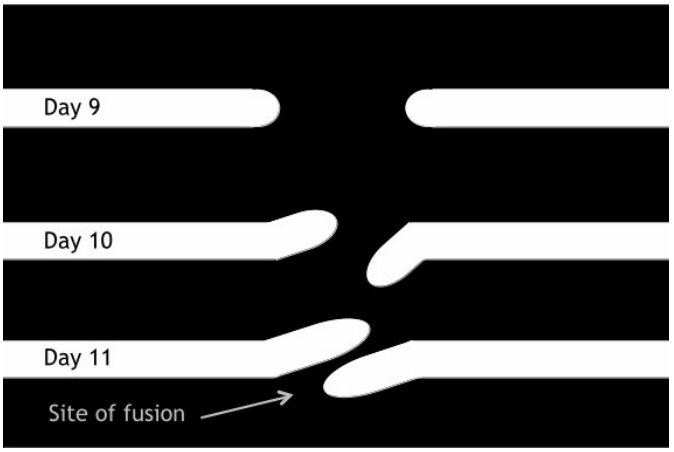

FIGURE 1.1: Schematic of approaching parabronchi over time.

phenotype to a complex branched cell with multiple cytoplasmic plates that are greatly attenuated [29, 46]. Reduction of the interstitial tissue allows the capillary endothelium and alveolar epithelium to approach, enabling formation of the thin blood-gas barrier [29].

In *Drosophila melanogaster*, epithelial fusion occurs via tracheal tip cells located at the ends of branches about to fuse. These cells extend filopodia to search for fusion targets, and eventually change cell shape to a seamless ring to allow for lumen passage. *D*E-cadherin, a cell adhesion molecule, accumulates at the site of contact, aiding in formation of a ring marking the site of lumen entry. *Escargot*, a zinc finger gene expressed in all tip cells, is also necessary here, as *escargot* mutant tip cells have been observed to not adhere normally. *Escargot* positively regulates *shotgun*, the gene responsible for producing *D*E-cadherin [43]. Assessing role of chicken *D*E-cadherin and *escargot* homologs may be an good start towards understanding epithelial fusion in birds.

1.4 Open Window Trials for *In Ovo* Manipulation

A major existing problem in the study of late-stage chicken embryos is the lack of accessibility to the embryo, which hinders the possibility of applying *in ovo*

interventions and observing the corresponding effects on lung development. If the lungs can be explanted and continue normal growth in culture, or if selected morphogens could be delivered to areas of growth in the lungs, it would greatly facilitate elucidation of the roles of morphogens identified thus far. In mammalian models, whole embryonic lungs are typically cultured in a mechanically supported culture format, and are historically grown on siliconized paper to provide flexible support and enable delivery of nutrients and signaling molecules to the bottom surface of the tissue, and optionally to the top surface [40].

A past study has attempted to culture Day 9 lungs on a thin layer of 3D Matrigel or a 2D Whatman membrane with pore diameter of 11μm, floating on Dulbecco's Modified Eagle Medium (DMEM) in 10% FBS. The lungs are incubated at 38°C and medium is replenished daily. However, after two days of growth on the 2D culture, the lungs are observed to be extremely flattened and are of significantly smaller size than normal Day 11 lung explants [17].

A proposed alternative is the open window approach, by which a portion of the eggshell is removed to allow access to the embryo, in the hopes that the embryo can still grow normally in the perturbed *in ovo* environment. Spurlin and Lwigale have developed a method of addressing the problem of the extraembryonic membranes that make experimental manipulations difficult past Day 5, including the issue of the amnion and chorion membranes fusing and surrounding the entire membrane by the time approach and anastomosis of adjacent sets of parabronchi occurs at Day 11.5. To solve this problem, Spurlin and Lwigale suggest removing 3-4 ml of albumen from Day 3 embryos with a syringe. As the eggs are then sealed with tape and incubated on their sides, this ensures no attachment of the embryo and extraembryonic membranes to the eggshell. At Day 5, the eggs are re-opened and the amnion and chorioallantoic membranes are dissected away from the embryo [42]. Although this is procedure was developed for final dissection around Day 8, this does provide a potentially feasible way to gain access to the embryo and in particular its vasculature, into which interventions can be injected. A modified version of this procedure will be evaluated to see if it is a viable solution for the *in ovo* manipulation problem for Day 11-12 chicken embryos.

1.5 Slug Zinc Finger Transcription Factor

A number of molecules are thought to be involved in the avian program of lung branching morphogenesis (although their precise roles are still unclear), including TGFβ, SHH, and FGF10. However, unlike these molecules, Slug, an intracellular zinc finger transcription factor in the Snail protein family, is thought to localize in the lung mesenchyme at higher concentrations in the regions between the tips of approaching parabronchi, right before anastomosis occurs at Day 11.5 [17]. As this study will focus on this anastomosis event, Slug is a particularly relevant target molecule for open window interventions.

In avian heart systems, Slug is involved in the formation of mesoderm, particularly in the process of EMT. It is thought to be a marker for epithelial cells that are competent to undergo the transition to mesenchymal cells [6]. The involvement of Slug in EMT is, more specifically, due to its ability to cause desmosomal dissociation, a first step that begins the process of converting from an epithelial to a mesenchymal phenotype [36]. Slug exerts its invasion-promoting effects in human cell lines by repressing E-cadherin transcription. The avian homolog of E-cadherin is LCAM, which is a prominent molecule targeted in immunostaining in this study. This invasion is suppressed by p53, a tumor suppressor gene that induces Slug degradation [41]. A candidate molecule for use as an intervention in open window studies is GN25, a p53-Snail binding inhibitor [39]. Inhibiting p53-Snail binding may lead to a higher concentration of Slug (a Snail-family protein), which in turn could promote the invasion observed directly before anastomosis. The effects of GN25 and Slug on lung development are an important area for study via open window techniques.

Objectives

The first objective of this study is to further characterize the program of lung development in embryonic chickens. In particular, this study focuses on the profuse parabronchial fusion observed between Days 11 and 12 that enables continuous airflow and allows an increase in gas exchange efficiency in avians. This is accomplished by explanting chicken lungs after an appropriate amount of growth, staining for a variety of relevant cellular markers, and analyzing the results by epifluorescent microscopy.

The second objective of the study is to contribute to the ongoing quest to fully understand the program of lung branching morphogenesis in chickens by assessing the viability of *in ovo* manipulations to molecules present in the lung environment. Within the scope of this study, the aim is to attempt to elucidate the role of molecules such as Slug, an intracellular zinc finger transcription factor in the Snail family [6], that has been shown to be present in higher concentrations between two parabronchi directly before anastomosis at Day 11.5 [17]. Two open window approaches will be pursued and their viability compared.

The final objective of this study is to gain insight as to whether a reaction-diffusion system may be an appropriate model for the observed program of branching morphogenesis, particularly with regards to the approach and fusion of opposing sets of parabronchi. This will be done by comparing the distances between approaching parabronchi when growth patterns change to the distances over which morphogens act in existing proposed models for reaction diffusion systems.

Materials and Methods

3.1 Hamburger-Hamilton Staging and Incubation

Hamburger-Hamilton (HH) stages are assigned to embryonic chicken lungs prior to dissection [16]. Features used to distinguish between stages are feather germ development, beak size, eyelid coverage, and development of extremities. Day 11 embryos typically correspond to HH37, while Day 12 embryos correspond to HH38. Little variation is observed in this correlation. White Leghorn chicken (*Gallus gallus* variant *domesticus*) eggs are first put into the incubator at 38°C with automatically tilting shelves between 10AM and noon to ensure regular timing of fusion. Eggs dissected on Day 11 after 6PM are referred to as Day 11.5, and correspond to an intermediate HH stage, called HH38.5. Dissections primarily occurred on Day 11 (HH37) and Day 12 (HH38), but ranged from Day 9 (HH35) to Day 14 (HH40) in order to better characterize the larger picture of lung branch development and fusion.

3.2 Lung Explantation and Immunofluorescent Staining

Whole lungs are dissected out of the chicken embryos in a solution of phosphate-buffered saline (PBS) and fixed in a 4% paraformaldehyde in PBS solution for 15 minutes. The lungs are washed 3 times for 15 minutes per wash in a solution of

PBS with 0.3% Triton-X-100 (PBST), and are then blocked in 10% goat serum in PBST for 4 hours. A shaker is used for each of these steps. The lungs are then incubated at 4°C overnight in a primary antibody dilution. The primary antibody dilutions used are shown in Table 3.1, and are based on previous immunostaining work [17].

TABLE 3.1: Primary antibody dilutions used for the lung staining procedure.

Target Molecule	Primary Antibody Dilution
LCAM	1:100
Slug	1:500
β-Catenin	1:2000
DAPI	1:1000
Vimentin	1:1000

Following overnight incubation in primary antibody, lungs are washed 5 times for 15 minutes each on a shaker in a solution of PBST. Lungs are then again incubated overnight at 4°C, this time in a 1:500 dilution of Alexa 594 goat-anti-mouse. In cases where a double-stain is performed and one of the primary antibodies is rabbit-derived, Alexa 488 goat-anti-rabbit is used. Finally, the lungs are washed 3 more times in PBST, at which point they are ready for epifluorescent imaging. A shaker is again used for all of these steps. The lungs are placed in 24-well plates for all of these staining and washing steps, and the plates are wrapped in tin foil after addition of the Alexa secondary antibody to minimize loss of fluorescence. Prior work has further dehydrated the lungs with isopropanol and imaged samples in a solution of Murray's clear (2:1 benzyl benzoate:benzyl alcohol). However, although this method was attempted, the images obtained via imaging in PBST were determined to be better and of an acceptably high quality [17].

3.3 Epifluorescent Imaging and Image Processing

A Hamamatsu ORCA digital charge-coupled device camera attached to a Nikon Eclipse Ti-S fluorescent microscope is used to image whole lungs, with either 2x,

4x, 10x, or 20x objectives. The lungs are imaged in the same 24-well plates used during the staining step, submerged in a PBST solution. Fluorescent light intensity and exposure time are varied to obtain adequate brightness and contrast in the images. If the lungs are too large for the 2x objective, and particularly in cases where both lobes of the lung are still attached to the trachea, multiple images are taken and merged as needed using the Mosaic feature available in Fiji software.

3.4 Open Window Trials

3.4.1 Maximal Access Procedure

The Maximal Access (MA) procedure for open window experiments is adapted from the methods described by Korn and Cramer, optimized for long survival times, and from the methods described by Spurlin and Lwigale, designed for later stage embryos [21, 42]. On the morning of Day 11, the exterior of the eggshell is disinfected by light application of betadiene. Tape is applied to the egg to stabilize the shell, and a small, circular hole is cut through the shell and tape on the side of the egg. Using a B-D 30G PrecisionGlide needle and a 1mL syringe, the selected intervention is injected directly into the exposed vasculature of the embryo. The possible interventions are the control (no injection), ROCK inhibitor Y-27632, and Slug inhibitor GN25. After the injection is complete, eggshell is resealed with tape, and the egg is placed in a second incubator, also at 38°C and the same humidity, but without tilting to minimize loss of albumen. At Day 12, the tape is removed and the embryos are dissected following the normal lung explantation and staining procedure described above.

3.4.2 Minimal Invasion Procedure

The Minimal Invasion (MI) procedure is adapted from the MA procedure previously described and is intended to provide access to intact vasculature without damaging the blood vessels or the embryo. This is accomplished by first examining the intact egg under a bright light source to locate the position of vasculature running along the inner surface of the eggshell. A small square is marked in pencil around a region that encompasses a large blood vessel. The eggshell exterior is disinfected with light application of betadiene. A razor is used to delicately cut away at the exterior eggshell. This must be done slowly and carefully to avoid breaking open the egg. The exterior eggshell is removed, revealing the thin interior eggshell and the blood vessel underneath. Using the same injection procedure as in the MA procedure, the intervention is slowly injected directly into the bloodstream to minimize rupturing. After injection, the eggshell is resealed and the egg is placed in a second incubator just as in the MA procedure.

3.4.3 Analysis of Parabronchial Approach and Fusion

The distances between approaching parabronchial tips at HH35 to HH40 are measured in pixels in Fiji using images of lungs stained for LCAM. The pixels are converted to distances derived from the size of the field of view for each objective. As lung specimens did not lie flat under the microscope, accurate whole lung measurements were difficult, so normalization of distances was not done. This point is accounted for in the interpretation of the results.

Opposing parabronchi are paired in groups of two for the sake of measuring angle of deflection preceding anastomosis. Images from HH37 and HH37.5 are used to measure angle of deflection, defined as the angle by which direction of actual growth deviates from the direction of growth projected by prior development of the parabronchus. This occurs to allow interlocking with the opposing set of parabronchi. The angle of deflection is measured in Fiji, and pairs of angles of deflection are plotted against each other.

Results

4.1 Characterization of Parabronchial Approach and Fusion

This section describes the branching morphogenesis observed in late stage embryonic chicken lungs. Analysis focuses in on a region at which profuse anastomosis occurs at HH38, named the Ridge of Anastomosis (ROA) for the purposes of this study. This event is partially responsible for enabling the continuous air flow characteristic of avian lungs. The ROA features opposing sets of roughly parallel parabronchi that steadily approach each other, interweave slightly, and fuse. The pattern of growth will be described, along with quantitative analysis of the distance between approaching parabronchi and angle of deflection during interweaving.

4.1.1 Qualitative Analysis of Parabronchial Growth and Fusion

LCAM is the avian homolog of E-cadherin, a cell adhesion protein present in the epithelial tissue, and is the accepted way to identify epithelial tissue patterning. In the case of the embryonic chicken lung, staining for LCAM allows for visualization of the growing parabronchi at various stages, and is also conducive for high-magnification imaging of epithelial fusion events. To more definitively map

out the program of parabronchial growth, branching, and fusion, lungs from HH35-HH42 (Day 9 to Day 16) were immunostained for LCAM, focusing in on events happening at the ROA.

At HH35-36, sets of roughly parallel parabronchi are consistently observed to be steadily approaching each other following several bifurcation events (see Figure 4.1). Growth rate is fairly consistent across all parabronchi in this region, and individual pairs of approaching parabronchi reach each other at similar times.

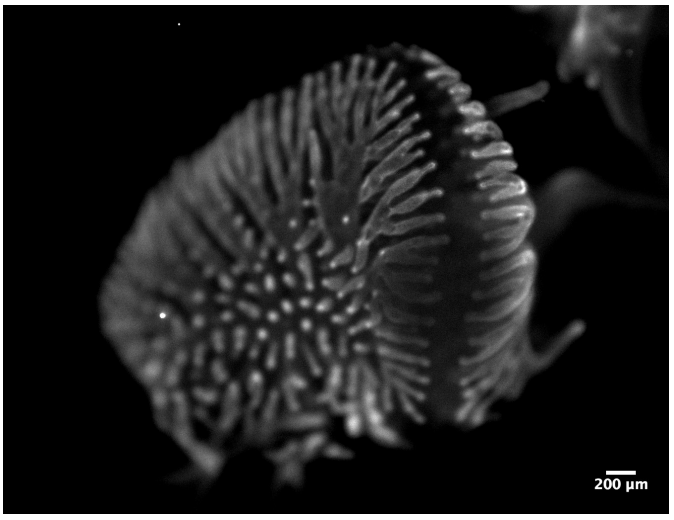

FIGURE 4.1: Epifluorescent image at 2x objective of HH35 (Day 9) embryonic chicken lung parabronchi stained for LCAM. The area of approaching sets of parabronchi is the region of interest.

At HH37, opposing parabronchi have gotten close enough that they begin to change direction of growth in order to begin to interweave with the opposing set of parabronchi, as seen in Figure 4.2 on the next page. Direct collision and fusion at the nearest point is not observed. It is not clear whether this is a monopodial branching event or simply a change in direction of growth. In any case, this result suggests presence of a signaling mechanism operating between epithelial tissues through the mesenchymal tissue by which parabronchi are informed of the location of approaching parabronchi and are able to adjust direction of growth such that direct collision does not occur.

Starting after HH37, profuse anastomosis begins to occur at the ROA. To properly characterize this event, another Hamburger Hamilton stage, HH37.5 (Day 11.5)

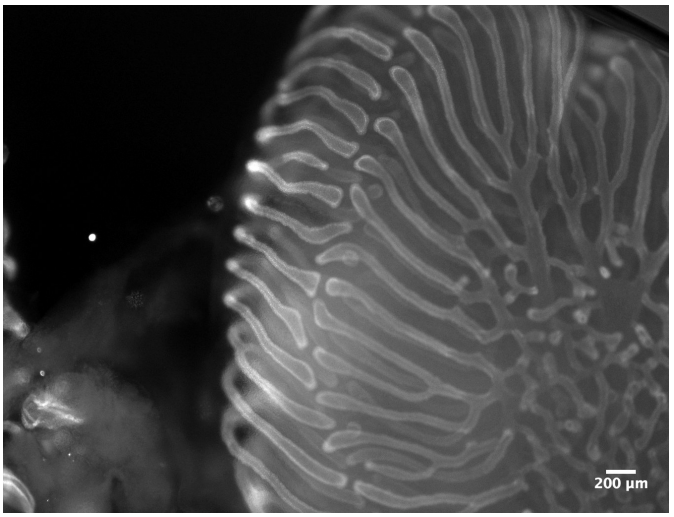

FIGURE 4.2: Epifluorescent image at 2x objective of HH37 (Day 11) embryonic chicken lung parabronchi stained for LCAM, showing the change in direction of parabronchial growth to ensure interweaving.

is defined between HH37 and HH38. At HH37.5, the directional change seen at HH37 is still observed (see Figure 4.3), with a progression in interweaving of the parabronchi. At this point opposing parabronchi have large areas running parallel to each other. Additionally, at this point a possible monopodial branching event is observed, as growth is observed beginning 200-400μm down from the epithelial tip and progressing in the direction of the opposing adjacent parabronchus.

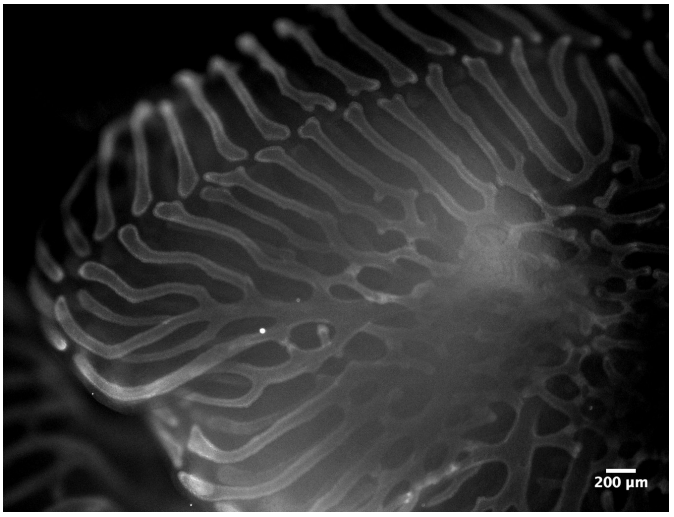

FIGURE 4.3: Epifluorescent image at 2x objective of HH37.5 (Day 11.5) embryonic chicken lung parabronchi stained for LCAM, showing interweaving of parabronchi and possible monopodial branching.

At this point, fusion begins to occur between adjacent approaching parabronchi

via growth from both sides across the mesenchymal gap. It is clear that no lumen has yet begun to develop. However, a bridge of epithelial tissue has developed between the opposing parabronchi, as seen at high magnifications in Figures 4.4 and 4.5.

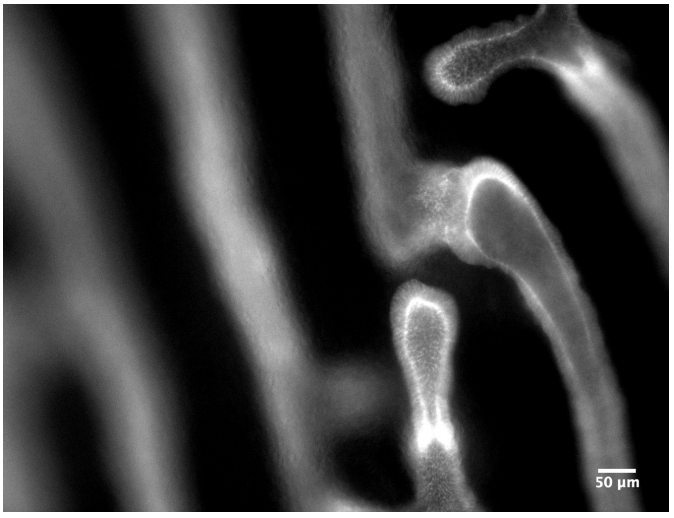

FIGURE 4.4: Epifluorescent image at 10x objective of HH38 (Day 12) embryonic chicken lung parabronchi stained for LCAM, focusing in on the novel fusion between opposing parabronchi that occurs at this stage.

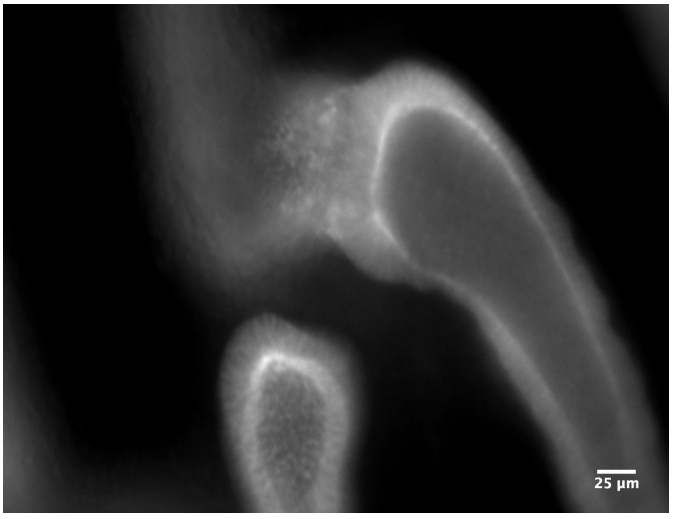

FIGURE 4.5: Epifluorescent image at 20x objective of HH38 (Day 12) embryonic chicken lung parabronchi stained for LCAM, showing more detail of the epithelial fusion at high magnification.

After HH38, anastomosis continues and the epithelial bridge between opposing parabronchi strengthens. By HH39 and HH40, anastomosis is nearly complete across the entire ROA. At this point, it is possible to observe very small protrusions along the sides of some parabronchi, far away from the site of fusion, as seen in

Figure 4.6. As discussed later in Figure 4.11 on page 24, these develop into evenly spaced protrusions across the entire parabronchi network. These protrusions are discussed later in more detail, and are a subject for future studies.

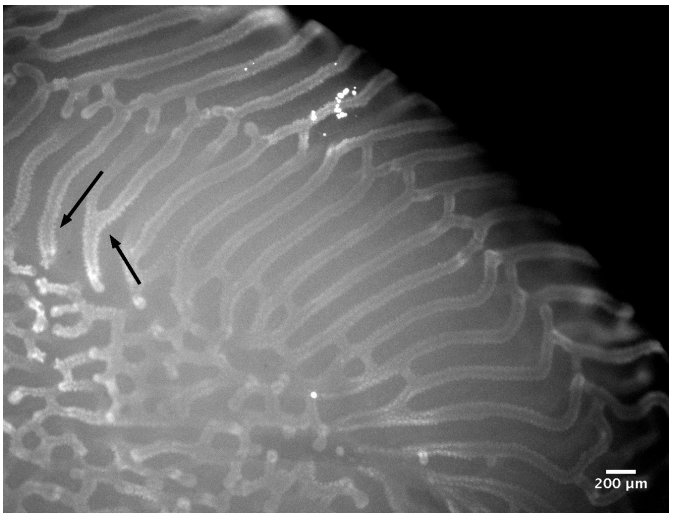

FIGURE 4.6: Epifluorescent image at 2x objective of HH39 (Day 13) embryonic chicken lung parabronchi stained for LCAM. Profuse anastomosis has occurred at the ROI, and small protrusions can be observed along the sides of some parabronchi, as indicated by the arrows.

4.1.2 Distances Between Approaching Parabronchi Over Time

To quantify the growth of parabronchi before, during, and after formation of the ROA, the distance between approaching adjacent parabronchi was measured (i.e. the distance between the tip of a parabronchus and the closest point on a parabronchus in the opposing set). The distances measured are shown in Figure 4.7 on the next page, where a distance of zero indicates that anastomosis has occurred for that particular set of two parabronchi.

As this study primarily focused on the initiation of the anastomosis events between HH37 and HH38, there was no data available for HH36, as images taken at HH35, HH39, and HH40 had been carried out for the sake of exploratory analysis. However, given the obvious progression of sets of parabronchi towards each other at the ROA in all lungs imaged, it is near certain that the distances at HH36

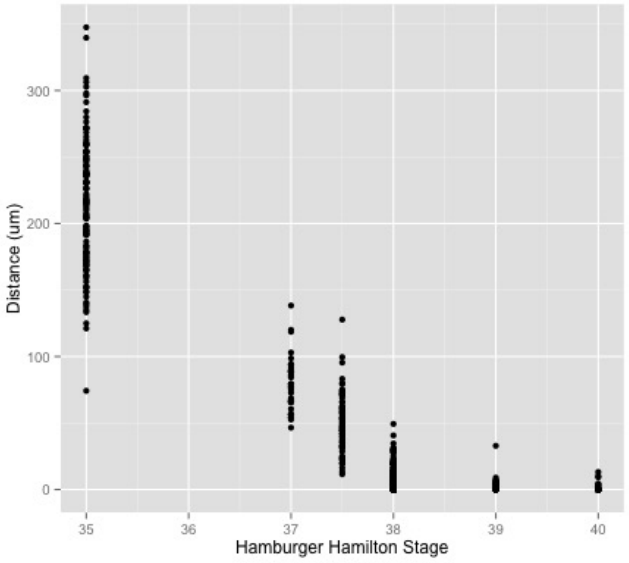

FIGURE 4.7: The closest distance between parallel sets of approaching parabronchi in μm is shown from HH35 to HH40. Distance steadily decreases as parabronchi grow towards each other and profuse anastomosis occurs.

would fall in between the distances measured for HH35 and HH37. The summary of the distance measurements, including number of measurements, mean distance, and the % of pairs that have undergone anastomosis, is shown in Table 4.1.

TABLE 4.1: Summary of distance measurements made for lungs at various HH stages.

HH Stage	# Of Measurements	Mean Distance (μm)	% Anastomosis
35	128	214.65	0%
37	46	78.40	0%
37.5	76	50.37	0%
38	249	7.35	59.03%
39	81	1.50	74.07%
40	65	0.74	87.69%

In interpreting these results, it is worth noting that the lungs as a whole grew in size from HH35 to HH40. However, as the lungs did not have to be cleared for adequate imaging, in many cases the lungs did not lie flat under the microscope. Therefore, it was not practical to measure lung diameters and report distances as a fraction of total lung diameter. As expected, the distance between approaching parabronchi consistently decreases from HH35 to HH40. Anastomosis is not first observed until HH38, when the proportion of parabronchi anastomosed rapidly

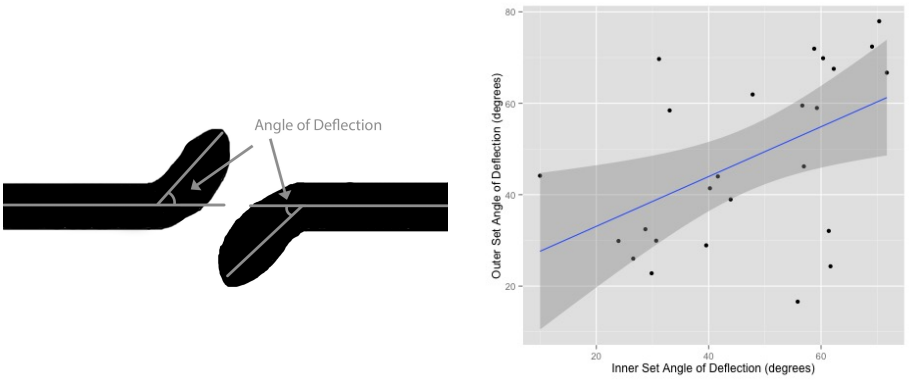

FIGURE 4.8: An angles of deflection pair is defined in the schematic on the left. The chart on the right shows the angles of deflection pairings by which actual growth deviates from projected growth. Inner set indicates the set of parabronchi closer to the lung's inner face (where the trachea connects), while the outer set is the opposing set originating from the lung's outer face.

jumps from 0% to 59.03%. This suggests that the mechanism for fusion across these adjacent sets of parabronchi may be coordinated in some way, and this result may be used to guide further exploration along this path.

4.1.3 Parabronchial Angle of Approach

To assess the effect of location of opposing parabronchi on growth, the angles of deflection of pairs of approaching parabronchi were measured. The angle of deflection is defined as the angle of deviation from which actual growth at HH37-HH37.5 differed directionally from that projected at earlier stages. The angles of deflection in 25 pairs of parabronchi (2 angles per pair) were measured and the pairs are shown in Figure 4.8.

The figure includes a linear regression line of best fit, and the shaded region indicates the 95% confidence interval. The results indicate that if the angle of deflection is high in one parabronchus in an opposing set of two, it is usually high in the other parabronchus in the set as well. This supports the observation that parabronchi deflect in order to allow for slight interweaving prior to fusion. In situations where parabronchi are lined up closely, both typically exhibit large angles of deflection to ensure that a premature collision is avoided.

4.2 Target Molecule Immunostain Analysis

In the following subsections, the relevance of staining for each target molecule will be mentioned, along with the relative success or failure of imaging and staining for each one. The information on the program of branching morphogenesis gleaned from each type of stain will be discussed as well.

4.2.1 β-catenin

β-catenin is an intracellular protein thought to be involved in EMT, specifically via a crosstalk regulatory mechanism involving promotion of BMP4 (bone morphogenetic protein 4) and FGFR2 (FGF receptor 2) expression in the mesenchyme [32]. It has dual functions in cell adhesion and Wnt signaling, and forms cell adhesion complexes with LCAM in the epithelium of chicken lungs to ensure structural integrity of epithelial tissue. Its role in the Wnt signaling pathway indicates that it is a potential driver of cell growth as well, and chronic activation of β-catenin is thought to be a potential cause of cancer [2].

Immunostains for β-catenin localization patterns were conducted in this study both to confirm the epithelium patterns indicated by prior LCAM stains (as the two form cell adhesion complexes) and to potentially suggest involvement of β-catenin in subsequent growth (as it is involved in the Wnt signaling pathway). Whole chicken lungs explanted at HH37, HH37.5, and HH38 (Day 11, 11.5, and 12) were stained using a mouse-derived β-catenin primary antibody and imaged at low and high magnifications under the epifluorescent microscope.

The β-catenin immunostains (some of which are shown in Figures 4.9 on the following page and 4.10 on the next page) confirm the shape and organization of parabronchi at HH37-38 that had been indicated by LCAM staining. The parallel sets of approaching parabronchi are again observed, with each parabronchus of comparable length and width to that seen thus far. Furthermore, the images lend support to the possibility that β-catenin may be involved in epithelial growth,

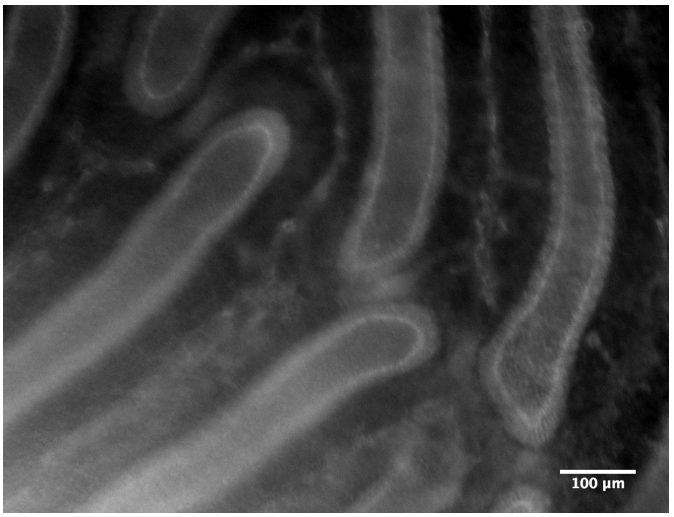

FIGURE 4.9: Epifluorescent image at 10x objective of HH37.5 (Day 11.5) embryonic chicken lung parabronchi stained for β-catenin, focusing in on β-catenin localization along the ridge of anastomosis.

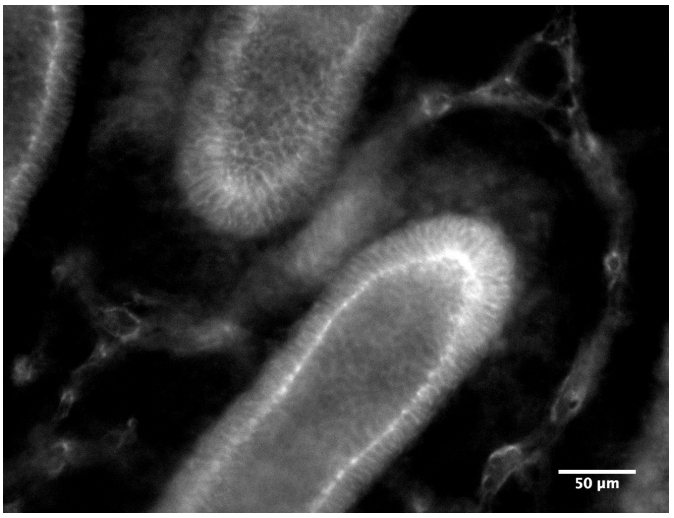

FIGURE 4.10: Epifluorescent image at 20x objective of HH37.5 (Day 11.5) embryonic chicken lung parabronchi stained for β-catenin. Higher magnification image of approaching parabronchi about to undergo fusion.

as not only does β-catenin appear to be slightly more concentrated along the epithelial tips, but it is also clearly present in the space between approaching epithelial tips as anastomosis is about to occur. More rigorous analysis of β-catenin localization in a higher volume of chicken lungs, along with open window trials involving intervention with a β-catenin inhibitor are two areas for further analysis that will help to further elucidate the role of β-catenin in epithelial growth.

4.2.2 Late Stage Epithelial Protrusions and LCAM/DAPI Double-staining

Prior to this study, little was known about epithelial development in later stage embryonic chicken lungs. To begin to further understand parabronchial development following the profuse anastomosis observed between HH37 and HH38, lungs at HH40 and HH41 were immunostained for LCAM and imaged via epifluorescent microscope. The result was unexpected, as novel small-scale epithelial protrusions were observed along established parabronchi, indicating a potentially entirely new mechanism of branching that had yet been unobserved and uncharacterized.

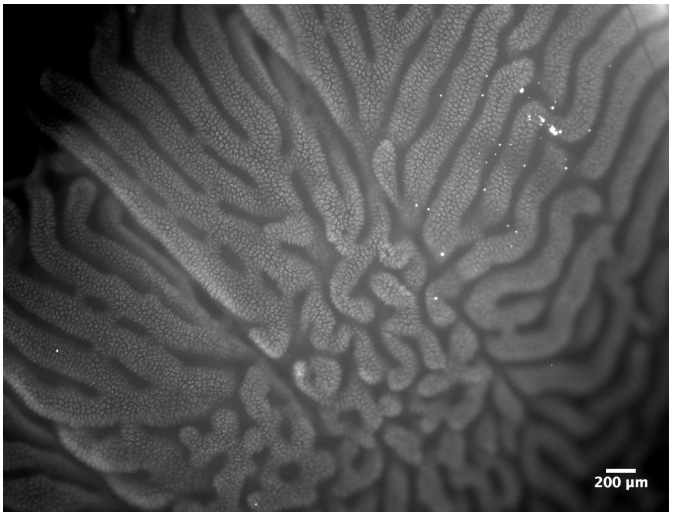

FIGURE 4.11: Epifluorescent image at 2x objective of HH41 (Day 15) embryonic chicken lung stained for LCAM indicating small-scale epithelial growth in a previously unobserved pattern of growth.

As seen in Figure 4.11, the epithelial protrusions are small and appear to be regularly spaced throughout the parabronchi. The normal linear parabronchi border between epithelium and mesenchyme is now harder to distinguish, suggesting that the protrusions are likely occurring perpendicularly (out of the page in Figure 4.11) to previous modes of branching and growth. Although the end result and function of this small-scale growth is still unknown, the cross-current gas exchange functionality of lung parabronchi suggests that the purpose of this growth may be to increase parabronchial surface area, improving the capacity for gas exchange.

To help determine the nature of the late stage epithelial projections, 4' 6-diamino-2-phenylindole dihydrochloride (DAPI), a molecule commonly used to stain nuclear chromosomal DNA, was used in HH38-HH40 lungs. Specifically, 4 lung lobes at HH39, 2 lung lobes at HH40, and 4 lung lobes at HH41 were successfully double-stained for LCAM and DAPI. This was accomplished using a goat-derived LCAM primary antibody and a mouse-derived DAPI primary antibody.

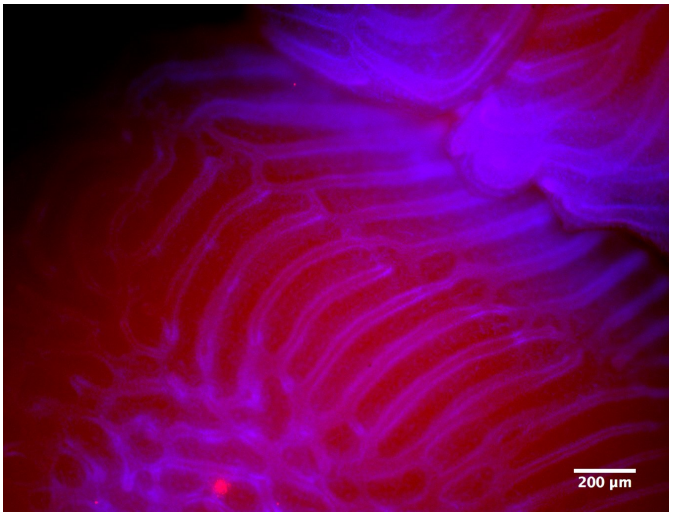

FIGURE 4.12: Epifluorescent image at 4x objective of HH40 (Day 14) embryonic chicken lung double-stained for LCAM (blue) and DAPI (red).

As shown in Figure 4.12, the DAPI/LCAM double-stains were difficult to interpret, but suggested that nuclear DNA is not co-localized with the small-scale epithelial protrusions along the parabronchial epithelium. These protrusions have not been explored in depth, and are a potential subject for further exploration. Such inquiry would require epifluorescent imaging of lungs past Day 15 to allow for observation of the progression of the protrusions and determination of whether they develop into sub-parabronchi epithelial structures.

4.2.3 Slug

As previously discussed in Section 4.2.3, Slug is a zinc finger transcription factor in the Snail protein family, and is known to be present in higher concentrations in the mesenchyme directly between approaching parabronchi before fusion events [17]. It is involved in EMT, and is thought to be a marker for cells about to

undergo transition to mesenchymal cells. One goal of this study is to further evaluate the role of Slug in epithelial fusion. A series of lungs at HH37-HH38 were immunostained for Slug for the sake of attempting to confirm a similar concentration pattern as that observed in prior work [17].

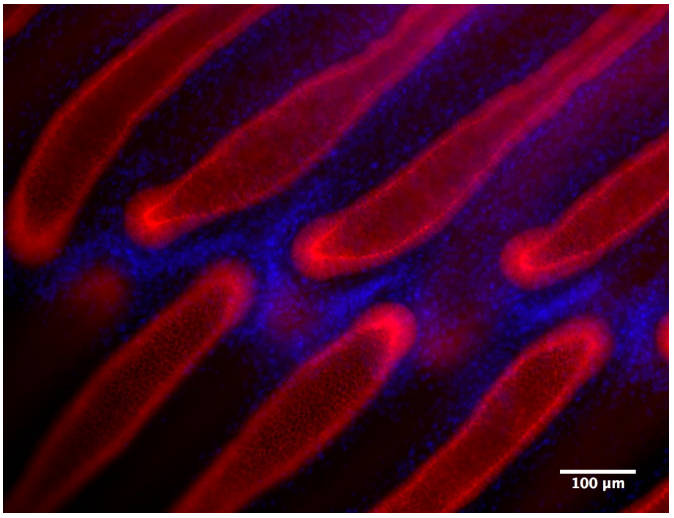

FIGURE 4.13: Epifluorescent image at 10x objective of HH37 (Day 11) embryonic chicken lung double-stained for LCAM (red) and Slug (blue).

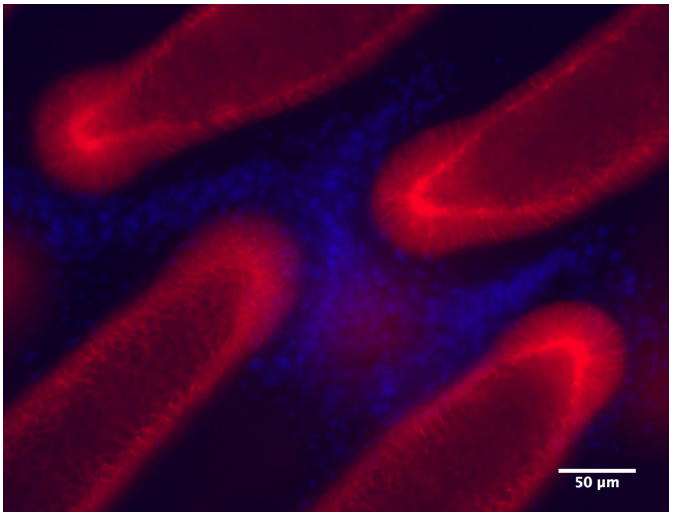

FIGURE 4.14: Epifluorescent image at 20x objective of HH37 (Day 11) embryonic chicken lung double-stained for LCAM (red) and Slug (blue).

The expression pattern shown in Figures 4.13 and 4.14 is far more clear than that seen in studies to this point. The Slug protein is clearly expressed in greater concentration in mesenchymal cells that are adjacent to the tips of growing epithelium, and in particular directly between sets of approaching tips that are about to undergo anastomosis. Concentration of Slug decreases rapidly as distance from

epithelium increases, and it is hardly seen in mesenchymal cells that are more than 20μm away from the epithelium.

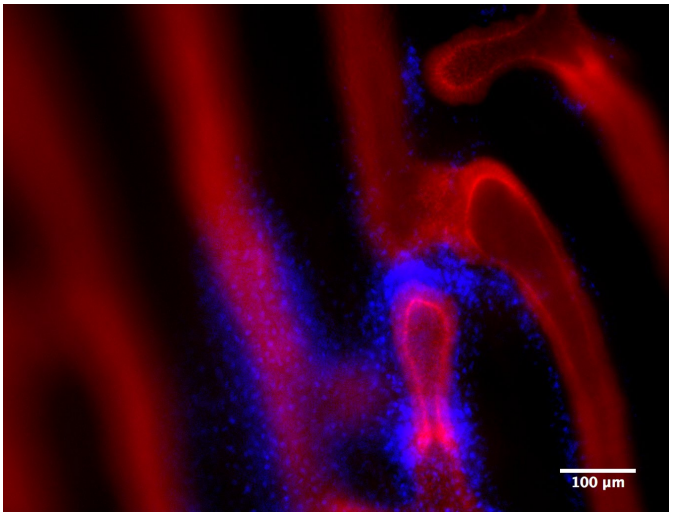

FIGURE 4.15: Epifluorescent image at 10x objective of HH38 (Day 12) embryonic chicken lung double-stained for LCAM (red) and Slug (blue).

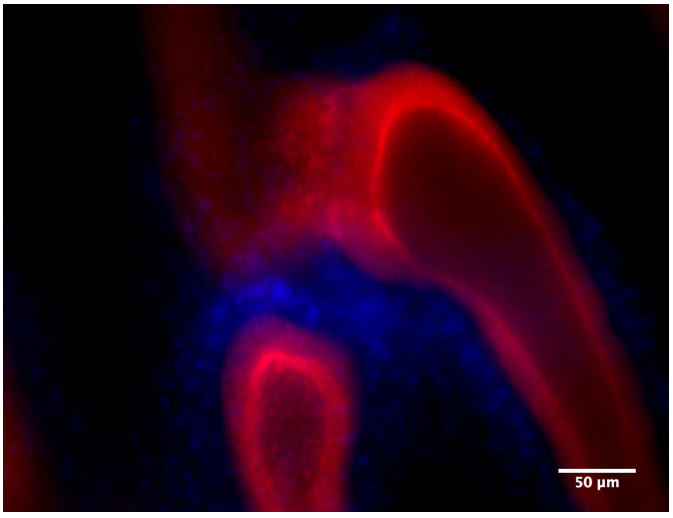

FIGURE 4.16: Epifluorescent image at 20x objective of HH38 (Day 12) embryonic chicken lung double-stained for LCAM (red) and Slug (blue).

HH38 (Day 12) lungs were double-stained for Slug and LCAM as well, as seen in Figures 4.15 and 4.16. At this point, the process of epithelial fusion is underway, and the Slug-rich mesenchymal environment between tips of approaching parabronchi that was observed at HH37 is gone. Instead, Slug is still localized in mesenchyme that is adjacent to epithelial tissue, with particularly high concentration in the mesenchyme alongside areas of fusion, where the epithelial tips once were. Additionally, it is worth noting that in Figure 4.15, it appears that Slug

may be present in the epithelium as well, since areas of epithelium are observed to be blue. However, it is likely that in this case, the Slug molecules observed by the stain reside in the mesenchyme above the underlying epithelium, and are not actually in the epithelium. Further imaging efforts of this double-stain combination using a confocal microscope focused to the appropriate set of z-stacks would definitively confirm or deny this, and is an experiment that should be conducted in the future.

4.2.4 Vimentin

Vimentin, a protein in the intermediate filament family expressed in normal mesenchymal cells to maintain cellular integrity and provide stress resistance, is an EMT marker and was also targeted in immunostains in this study [35]. Overexpression of vimentin has been linked to tumor growth, and neo-expression of vimentin in the mesenchyme accompanies EMT in mouse mammary epithelial cells [14]. In this study, whole lungs at HH37 and HH38 were immunostained for vimentin, using a mouse-derived primary antibody. The procedure was attempted both with vimentin primary antibody dilutions of 1/200 and 1/1000. In both cases, after addition of the secondary antibody and imaging according to the normal procedure, the specimens appeared to express vimentin present nearly throughout the whole lung, and it was not possible to conclusively discern significant changes in mesenchymal concentration. It is possible that vimentin is present in significant concentration throughout the lung mesenchyme. However, further trials at even greater dilution of primary antibody are worthwhile and may better indicate concentration patterns of vimentin in the mesenchyme, particularly in relation to sites of growth and fusion at parabronchial tips.

4.3 Open Window Trials

A series of open window experiments were conducted in this study to begin to develop an experimental framework for solving the problem of accessibility to the

embryo, a problem that up to now had limited the capacity to explore the morphogenic functions of the molecules discussed thus far. This study evaluated two candidate open window procedures, a Minimal Invasion procedure and a Maximal Access procedure, assessing the feasibility and yield of both, as well as beginning to apply exploratory interventions, the results of which are described below.

4.3.1 Minimal Invasion (MI) vs. Maximal Access (MA)

The MI and MA procedures are described in Section 3.4. Both procedures were carried out on HH37 (Day 11) embryos, and the eggs were subsequently reopened and the lungs explanted at HH38 (Day 12). The MA procedure was attempted first and was found to have higher yield with regards to access, but inferior results in terms of successful interventions applied. In 14/16 (87.5%) MA trials, eggs were successfully windowed. However, a significant downside to this approach was that it did not leave vasculature intact, making it difficult to apply interventions. Thus, while the 7 embryos to which the control treatment was applied remained viable when the lungs were explanted at HH38, none of the trials involving application of an intervention were still viable when reopened at HH38. Since it was more difficult with the MA procedure to identify and access intact vasculature, the chosen injection site with this procedure was closer to the embryo. Additionally, injections attempted here were higher volume (200-300μL), as a lower volume was expected to successfully enter the vasculature and make its way to the embryonic chicken lung. The volume and dilution of injections carried out will be discussed in more detail in Section 4.3.3.

Following the unsuccessful results obtained in the MA trials, MI open window experiments were also conducted. This procedure was more technically difficult and involved delicate work to remove eggshell without cracking the entire egg, so initial yield was lower, with 6/10 (60%) eggs successfully being windowed. However, this procedure kept all vasculature intact and maximized survival rate after application of an intervention. Once an appropriate dosage volume was injected, viable embryos were obtained at HH38, as will be discussed further in Section 4.3.3. It is

still possible that the MA approach is also feasible for late stage chicken embryos if further trials with varying intervention volume and concentration were attempted. However, for the purposes of this study and future work in this area, results indicate that the MI approach yields better results for the sake of comparing lung growth after application of various inhibitors to normal lung growth.

4.3.2 Control

After carrying out the MI open window procedure at HH37, lungs from a control group of four embryos were explanted at HH38 with only an intervention of 100μL of PBS applied. All embryos to which control treatment was applied survived until dissection (approximately 24 hours). The control group trials were conducted concurrently with the intervention trials to minimize variability of growth due to different intervention times, dissection times, or natural variability across batches of eggs. The average distance between approaching parabronchi at HH37 in the control group was 9.40μm (57 distances measured), which is reasonably similar to the average distance of 7.35μm (249 distances measured) for normal HH37 lungs. Furthermore, 43.9% (25/57) of approaching parabronchi had anastomosed in the open window control trials, compared to 41.0% (102/249) in normal HH37 lungs.

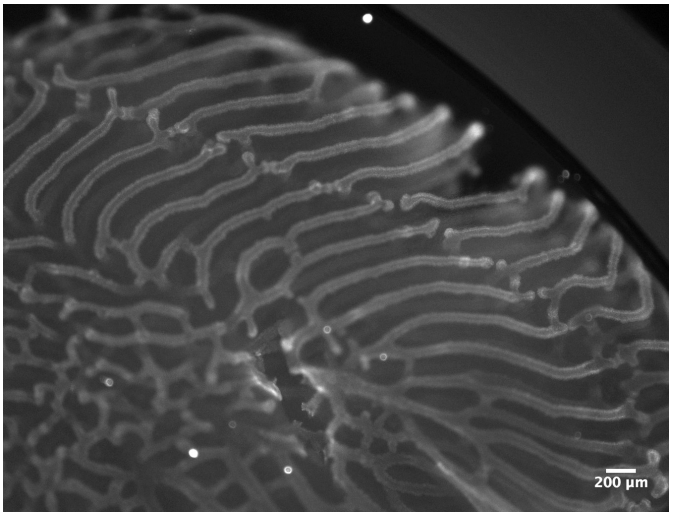

FIGURE 4.17: Epifluorescent image at 2x objective of HH38 (Day 12) embryonic chicken lung stained for LCAM following a Minimal Invasion open window procedure and control intervention.

Looking at the lungs subjected to the control treatment, one of which is shown in Figure 4.17 on the preceding page, there are no obvious and distinct differences in development between this lung and the normal HH38 lungs imaged previously. This qualitative result, along with the quantitative similarities in distance and proportion of parabronchi anastomosed, give no reason to believe that development in the control trial is different than that in lungs *in ovo*.

4.3.3 Validation of MI Intervention Approach

To validate that interventions applied via the MI approach were capable of causing changes in lung development of any kind, a "sledgehammer" approach was pursued. The rho-associated kinase (ROCK) inhibitor Y-27632 was chosen for this purpose. Rho-associated kinases interact with the cytoskeleton to regulate cellular contractility, motility, and morphology, so proper administration of Y-27632 intervention should significantly inhibit growth, if the MI approach is viable [1]. The ROCK inhibitor group consisted of four embryos. In all cases, a dilution of 1/100 Y-27632 in PBS was used. Varying the concentration of inhibitor is a subject for future trials. During the MI open window procedure, two of the embryos were injected with 200μL of Y-27632 via vasculature running along the inner surface of the shell that was exposed during the procedure. Two of the embryos were injected in the same manner with 100μL of Y-27632. In the former cases, both embryos died, and it could be observed that the vasculature was breaking due to the larger volume of liquid injected. In the latter cases, both embryos survived and were viable when dissected at HH38. One of the lungs imaged following Y-27632 treatment and explantation at HH38 is shown in Figure 4.18 on the next page.

Analysis of the lung images indicates an average distance between the tips of approaching parabronchi of 11.57μm (38 distances measured), which is both higher than the 9.40μm reported in the open window control group and the 7.35μm reported in normal HH38 lungs. However, 47.4% of approaching parabronchi had anastomosed, which is higher than the 43.9% recorded for the control group and the 41.0% recorded in normal lungs. A larger volume of trials with the Y-27632

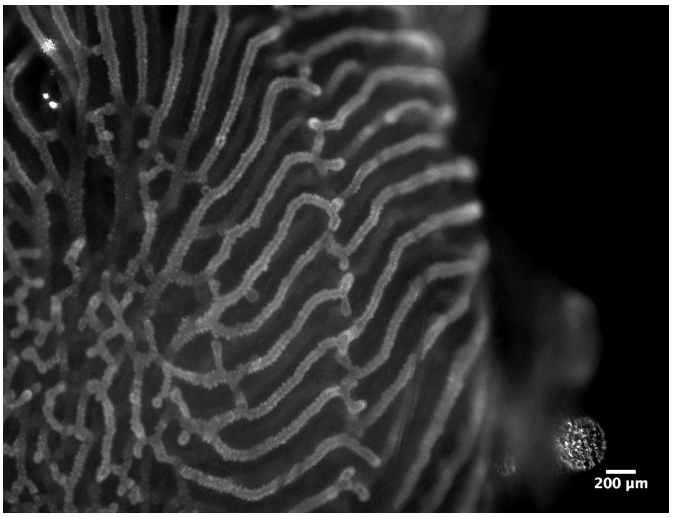

FIGURE 4.18: Epifluorescent image at 2x objective of HH38 (Day 12) embryonic chicken lung stained for LCAM following a Minimal Invasion open window procedure and intervention with 100μL of a 1/100 dilution of Y-27632 in PBS.

inhibitor at a variety of concentrations will be necessary to better assess the effects of the inhibitor on parabronchial growth and anastomosis.

4.3.4 Slug Inhibitor GN25 Intervention

Slug was identified as an initial target molecule for further exploration via repression/activation through open window trials due to its role in EMT. The immunostaining results confirmed its localization to mesenchymal cell adjacent to epithelium, in particular between epithelial tips about to undergo anastomosis between HH37 and HH38 (discussed in Section 4.2.3). GN25, a p53-Snail binding inhibitor (p53 induces Slug degradation), was obtained in order to test whether inhibition of p53-Snail binding would lead to higher Slug concentrations and increased promotion of invasion. Due to time constraints and the trial and error associated with developing and improving yield for novel open window procedures, intervention with GN25 has not yet been attempted, and will be a primary area for future work.

Discussion

5.1 Morphogenic Signaling Over Distances Measured in the Chicken Lung

As introduced in Section 1.2, although the patterns of epithelial branching, growth, and fusion observed in the embryonic chicken lung are quite complex, the program is highly stereotyped and the underlying rules governing patterning are likely very simple. This study focuses on the approach, interweaving, and subsequent fusion of opposing sets of parabronchi that occurs from HH37 to HH38. At HH37 and HH38, the parabronchi tips notably and consistently change direction of growth to avoid premature direct collisions with parabronchi from the opposing set. After slight interweaving occurs, both parabronchi grow towards each other and fuse their epithelial tissues in what may be a monopodial branching event that has only recently begun to be characterized [17].

As shown in Figure 4.8 on page 21, if one parabronchi has a high angle of deflection from the projected direction of growth, it is more likely that the other one does as well. That is, in cases where both parabronchi are directly lined up with each other, both experience a high angle of deflection to avoid a collision, a change in patterning that suggests presence of a long range inhibitor that directs growth above a certain concentration, as postulated by Turing [44].

A possible method of better evaluating this in the future is by using a set of partial differential equations for modeling lung reaction-diffusion systems proposed by

Meinhardt and adapting them to the geometry observed in the chicken lung [30]. These equations have been shown to be appropriate for human lung geometry and growth [15], but such a model has not been attempted in chickens. Adjusting the parameter values of this system will allow for more rigorous determination of whether this model can accurately represent epithelial growth, branching, and fusion in chicken lungs.

The distance measurements carried out in this study provide initial support for the possibility of control being under such a reaction-diffusion mechanism. At HH37 to HH37.5, none of the parabronchi have anastomosed yet, and the mean distance between opposing parabronchi is 78.40μm and 50.37μm for HH37 and HH37.5, respectively. It is important to first note that these distances are comparable to those reported in past work for parabronchial development at this stage [17]. Furthermore, past studies that have examined the roles of morphogens in lung geometries have also analyzed signaling over similar distances (50-100μm) as those reported in this study.

For example, a Bellusci *et al.* study investigating the role of FGF10 by characterizing its expression patterns in early stages in the development of the mouse lung suggests that the morphogen may direct new budding in the lung epithelium, and that concentration is dependent on location of prior buds. The distance between adjacent buds is consistently on the same order of magnitude (around 50μm) as the measurements reported in this study [3]. Additionally, Hagiwara *et al.*'s study adapting Meinhardt's partial differential equation for the geometry of human lungs reports pattern formation for both the model and observed cell cultures of normal human bronchial epithelial cells at distances less than 200μm, further supporting the relevance of a reaction-diffusion model for development chicken lung parabronchi [15]. Attempting to adapt reaction-diffusion equations to the growth patterns observed in avian lungs is an important next step to be able to understand the control mechanism and further elucidate the roles of the various morphogens in this environment.

5.2 Immunostains of Select Target Molecules

This study also carried out a series of immunostaining experiments for β-catenin, DAPI, Slug, and vimentin. Staining for β-catenin provided further evidence to confirm the epithelial patterning shown by earlier LCAM stains, as β-catenin functions in coordination with LCAM to form cell-adhesion complexes in the epithelium to ensure structural integrity [2]. The stains also indicated possible presence of β-catenin in the mesenchyme, particularly between the tips of parabronchi just before anastomosis occurs. As β-catenin was found both at slightly higher concentrations at the epithelial tips and in the mesenchyme where fusion subsequently occurs (see Figures 4.9 on page 23 and 4.10 on page 23), it is possible that the molecule has a role in marking sites along the epithelium for budding in preparation for fusion. β-catenin is also thought to be active in the promotion of BMP4 and FGFR2, as well as the Wnt signaling pathway, and is considered to be a potential cause of cancer if chronically activated, which supports the possibility that it is playing a function in growth of the chicken lung [2, 32].

As the DAPI stains exhibited widespread fluorescence due to the nuclear DNA target of the stain, DAPI/LCAM double stains were difficult to interpret, as seen in Figure 4.12 on page 25. DAPI did not seem to co-localize with the small epithelial protrusions observed at later stages and shown in Figure 4.11 on page 24. These very late stage protrusions have not yet been explored in previous studies, and are a good candidate for further exploration. Avian lungs are just 75% the size of comparably sized mammals by volume, yet they typically have 15% more surface area [26]. This massive increase in efficiency is one of the differences that allow birds to meet gas exchange needs at high altitudes, as the capacity for gas exchange is dependent on surface area available for gas exchange. It is possible that these small protrusions appearing in the parabronchi past HH40 function to dramatically increase the surface area of avian lungs available for gas exchange.

The Slug zinc finger transcription factor is known to be involved in EMT in other lung systems by causing desmosomal dissociation, a step that begins the conversion

from epithelial to mesenchymal phenotype [6]. The immunostaining experiments in this study showed clearly that Slug molecules were present at much higher concentrations in mesenchymal tissue directly close to epithelial tissue, and even more in mesenchymal tissue between epithelial tips that are about to undergo anastomosis (see Figures 4.13 on page 26 and 4.14 on page 26. This result made Slug a primary target for activation/inactivation in open window trials to further determine its role in morphogenesis, as discussed in more detail in Section 5.3.

Finally, several stains were carried out for vimentin, an intermediate filament protein expressed in mesenchymal cells that has been linked to EMT [35]. Although whole lungs at HH37 and HH38 were stained for vimentin using primary antibody dilutions of 1/200 and 1/1000, the efforts did not yield clear images, and it was difficult to determine any patterning in mesenchymal vimentin concentration. This is potentially due to presence of vimentin at higher concentrations compared to other target molecules throughout the lung mesenchyme. Further trials at greater dilutions are worth exploring in order to assess vimentin patterning, perhaps over time if possible, as neo-expression of the molecule has been observed to accompany EMT in mouse mammary epithelial cells [14].

5.3 Open Window Trials

A primary objective of this study was to develop a culture model or methodology by which growth of the late stage embryonic chicken lung could be imaged over time or by which the activity of various molecules could be manipulated and the resulting effects on growth determined. This has been a major problem hindering more extensive characterization of the chicken lung branching morphogenesis system to date. In mammalian models, mechanically supported cultures involving siliconized paper and nutrient delivery have proven effective for culturing whole embryonic lungs [40]. However, past efforts to culture late stage embryonic chicken lungs on 3D Matrigel or 2D Whitman membrane in nutrient medium have not been successful at maintaining lung volume, size and integrity [17].

The open window trials attempted in this study were an alternative approach at gaining the ability to manipulate activity of lung environment molecules in late stage lungs. Following a series of trials, the Minimal Invasion technique was determined to be superior to the Maximal Access technique for the sake of keeping vasculature intact and providing an effective site for injection. Future studies should employ the MI methodology in all cases where the intervention is an injection. The viability of this method was confirmed by injection of pure PBS to a control group, after which no significant change in lung development was observed.

To determine whether this type of intervention by injection into the vasculature was capable of effecting any sort of change in the development of the lung, it was necessary to conduct trials with a "sledgehammer" intervention. For this study, the ROCK inhibitor Y-27632 was used. Although only two trials were completed due to time constraints, initial results suggest that it's possible that growth was decreased due to the intervention, as the average distance between approaching parabronchi was 11.57μm, compared to 9.40μm for the control group. This difference is not statistically significant, as time constraints limited the number of Y-27632 open window trials to just 2, so conducting a higher volume of trials will be essential to better determine the viability of open window injection studies in this environment. These trials should explore the effects of a more comprehensive range of inhibitor dilutions beyond the 1/100 dilution carried out in this study.

The study established a framework to assess the role of molecules in the lung environment, specifically the role of Slug in branching morphogenesis and fusion. GN25 is a p53-Snail binding inhibitor. As p53 induces degradation of Snail, inhibition of p53-Snail binding can be expected to lead to higher Slug concentrations and increased promotion of invasion by repression of LCAM transcription [4]. These trials were not carried out in the present study due to time constraints, but rigorous pursuit of this line of exploration can serve as a framework for better assessing the roles of morphogens in the chicken lung environment using tools beyond just characterizing concentration gradients.

Conclusion

This study aimed to better characterize the program of lung development in embryonic chickens, focusing in particular on the profuse parabronchial anastomosis observed at the Ridge of Anastomosis between HH37 and HH38. This goal was achieved by immunostaining for LCAM followed by epifluorescent imaging of chicken lungs from HH35 to HH41, including a series of high magnification images of approaching sets of parabronchi directly before, during, and after fusion. The images obtained mark a significant improvement over all previous work done to characterize lung development in chickens. Immunostains for β-catenin and DAPI were carried out as well, suggesting possible involvement of β-catenin in epithelial growth, as well as indicating the presence of late-stage (HH39-41) small-scale epithelial protrusions that had never previously been observed. While the purpose of these protrusions discovered in the study remains unknown, it is possible that they function to increase surface area of lung epithelium and improve gas exchange capabilities, and are a subject for further exploration.

Additionally, the study sought to quantify growth of parabronchi before, during, and after formation of the Ridge of Anastomosis and to determine whether it was possible that the program of growth and fusion was under the control of a reaction-diffusion system. Approaching sets of parabronchi were organized in approaching pairs, and their angles of deflection measured. If one parabronchus in the set indicated a high angle of deflection, the other tended to exhibit a high angle of deflection as well, supporting the notion that growth patterns were influenced by the location of adjacent epithelium. The mean distance between opposing parabronchi at HH37 to HH37.5, the time prior to anastomosis at which direction

of growth is observed to change, is well within the distance range of 50-200μm at which morphogens have been thought to act in previous reaction-diffusion models developed for human and mouse lung geometries [3, 15].

Finally, the study sought to develop a viable experimental method of investigating the role of a number of molecules thought to be involved in morphogenesis through *in ovo* manipulation of the lung environment. This objective was accomplished by carrying out two open window procedures and assessing whether application of injection-based interventions was feasible in each case. The Minimal Invasion approach was determined to be superior to the Maximal Access approach, as all eggs to which the control PBS intervention was applied via this approach successfully survived 24 hours until dissection. While the Maximal Access approach was less technically difficult, it did not provide adequate access to the intact vasculature needed for application of the intervention, and was thus not further pursued. Initial trials with a "sledgehammer" intervention (ROCK inhibitor Y-27632) were carried out and early results indicate possible changes in growth pattern, which would support this technique as a viable way to explore the role of molecules in the lung environment *in ovo*. However, a greater volume of trials with Y-27632 would be required to determine this conclusively. Finally, Slug was identified as a candidate target molecule for future open window trials, as it was shown to localize in far greater concentrations in the mesenchyme directly between two approaching parabronchi in the site where fusion was about to occur.

Future Work

The primary area for future work is in further assessment of the viability of the MI open window procedure via "sledgehammer" Y-27632 ROCK inhibitor trials. Carrying out a larger volume of trials and experimenting with a range of inhibitor dilutions will allow researchers to more conclusively determine whether this procedure will be a viable framework for *in ovo* manipulations of molecules in the chicken lung environment. The measured distances between approaching parabronchi should be compared to those measured in the PBS intervention control group. If a significant difference is found between the two cases, manipulation of Slug activity via trials with GN25 p53-Slug binding inhibitor should be pursued. On a larger scale, if this experimental approach proves viable as promising early results from this study indicate it might, the MI open window procedure should be used as a framework for analyzing the role in growth and fusion of a variety of morphogens and other molecules in the lung environment. Aside from Slug, this should include manipulation of FGF10, SHH, TGFβ, and more.

As the distances between approaching parabronchi are within the range at which morphogens in reaction-diffusion systems have been thought to operate [3, 15], a second major area for future work is to see whether developing a reaction-diffusion model for chicken lungs is feasible. Although such models have been developed for the human lung geometry, none exist as of yet for chicken lungs, and would inform analysis of the role of lung morphogens. This work can be approached by taking the set of partial differential equations proposed by Meinhardt and used by Hagiwara to model human lung geometry and adapting them to chicken lung geometry [15, 30].

Bibliography

[1] Amano, M. ; Nakayama, M. ; Kaibuchi, K.: Rho-kinase/ROCK: A key regulator of the cytoskeleton and cell polarity. In: *Cytoskeleton (Hoboken)* 67(9):545-54 (2010)

[2] Barker, N. ; Born, M. van d.: Detection of beta-catenin localization by immunohistochemistry. In: *Methods Mol Biol* 468:91-8 (2008)

[3] Bellusci, Saverio ; Grindley, Justin ; Emoto, Hisayo ; Itoh, Nobuyuki ; Hogan, Brigid L. M.: Fibroblast Growth Factor 10 (FGF10) and branching morphogenesis in the embryonic mouse lung. In: *Development* 124:4867-4878 (1997)

[4] Bolós, V. ; Peinado, H. ; Pérez-Moreno, M.A. ; Fraga, M.F. ; Esteller, M. ; Cano, A.: The transcription factor Slug represses E-cadherin expression and induces epithelial to mesenchymal transitions: a comparison with Snail and E47 repressors. In: *J Cell Sci* 116(Pt 3):499-511 (2003)

[5] Calle, E.A. ; Ghaedi, M. ; Sundaram, S. ; Sivarapatna, A. ; Tseng, M.K. ; Niklason, L.E.: Strategies for whole lung tissue engineering. In: *IEEE Trans Biomed Eng* 61(5):1482-96 (2014)

[6] Carmona, Rita ; González-Iriarte, M. ; Macías, D. ; Pérez-Pomares, J.M. ; García-Garrido, L. ; Muñoz-Chápuli, R.: Immunolocalization of the transcription factor Slug in the developing avian heart. In: *Anat. Embryol. (Berl.)* 201(2):103-9 (2000)

[7] CDC: Chronic Obstructive Pulmonary Disease (COPD). In: *Centers for Disease Control and Prevention* (2015)

[8] Cieri, Robert L. ; Craven, Brent A. ; Schachner, Emma R. ; Farmer, C. G.: New insight into the evolution of the vertebrate respiratory system and the discovery of unidirectional airflow in iguana lungs. In: *Proc. Natl. Acad. Sci. USA* 111(48):17218-23 (2014)

[9] Combes, Alexander N. ; Short, Kieran M. ; Lefevre, James ; Hamilton, Nicholas A. ; Little, Melissa H. ; Smyth, Ian M.: An integrated pipeline for the multidimensional analysis of branching morphogenesis. In: *Nature Protocols* 9(12):2859-2879 (2014)

[10] Farmer, C. G. ; Sanders, Kent: Unidirectional Airflow in the Lungs of Alligators. In: *Science* 327(5963):338-340 (2010)

[11] Ghabrial, Amin ; Luschnig, Stefan ; Metzstein, Mark M. ; Krasnow, Mark A.: Branching Morphogenesis of the *Drosophila* Tracheal System. In: *Annu. Rev. Cell Dev. Biol.* 19:623-47 (2003)

[12] Gilbert, C.R. ; Smith, C.M.: Advanced lung disease: quality of life and role of palliative care. In: *Mt Sinai J Med* 76(1):63-70 (2009)

[13] Gleghorn, Jason P. ; Kwak, Jiyong ; Pavlovich, Amira L. ; Nelson, Celeste M.: Inhibitory Morphogens and Monopodial Branching of the Embryonic Chicken Lung. In: *Developmental Dynamics* 241(5):852-862 (2012)

[14] Gomez, Esther W. ; Chen, Qike K. ; Gjorevski, Nikolce ; Nelson, Celeste M.: Tissue geometry patterns epithelial-mesenchymal transition via intercellular mechanotransduction. In: *J. Cell. Biochem.* 110(1):44-51 (2010)

[15] Hagiwara, Masaya ; Peng, Fei ; Ho, Chih-Ming: In vitro reconstruction of branched tubular structures from lung epithelial cells in high cell concentration gradient environment. In: *Sci. Rep.* 5:8054. (2015)

[16] Hamburger, Viktor ; Hamilton, Howard L.: A series of normal stages in the development of the chick embryo. In: *Dev. Dyn.* 195(4):231-72 (1951)

[17] Huang, Siu-Yuan L.: Putting it together: a study of epithelial fusion in the avian lung. In: *Princeotn University Nelson Lab* (2014)

[18] Iber, D. ; Menshykau, D.: The control of branching morphogenesis. In: *Open Biol* 3(9):130088 (2013)

[19] Jones, Aled W. ; Radnor, Carolyn J. P.: The development of the chick tertiary bronchus. In: *J. Anat.* 113(Pt 3):303-24 (1972)

[20] Kim, Hye Y. ; Varner, Victor D. ; Nelson, Celeste M.: Apical constriction initiates new bud formation during monopodial branching of the embryonic chicken lung. In: *Development* 140:3146-3155 (2013)

[21] Korn, Matthew J. ; Cramer, Karina S.: Windowing Chicken Eggs for Developmental Studies. In: *J. Vis. Exp.* 8:306 (2007)

[22] Kotloff, R.M. ; Thabut, G.: Lung Transplantation. In: *Am J Respir Crit Care Med* 184(2):159-71 (2011)

[23] Locy, William A. ; Larsell, Olof: The Embryogy of the Bird's Lung. In: *American Journal of Anatomy* 19(3):447-504 (1916)

[24] Maina, John N.: Developmental dynamics of the bronchial (airway) and air sac systems of the avian respiratory system from day 3 to day 26 of life: a scanning electron microscopic study of the domestic fowl, Gallus gallus variant domesticus. In: *Anat. Embryol.* 207:119–134 (2003)

[25] Maina, John N.: Morphogenesis of the laminated, tripartite cytoarchitectural design of the blood-gas barrier of the avian lung: a systematic electron microscopic study on the domestic fowl, Gallus gallus variant domesticus. In: *Tissue Cell* 36:129-139 (2004)

[26] Maina, John N. ; King, A.S. ; Settle, G.: An allometric study of pulmonary morphometric parameters in birds, with mammalian comparisons. In: *Philos. Trans. R. Soc. Lond. B. Biol. Sci.* 326:1-57 (1989)

[27] Maina, John N. ; Woodward, Jeremy D.: Three-Dimensional Serial Section Computer Reconstruction of the Arrangement of the Structural Components of the Parabronchus of the Ostrich, Struthio Camelus Lung. In: *The Anatomical Record* 292:1685–1698 (2009)

[28] Makanya, A.N. ; Hlushchuk, R. ; Duncker, H.R. ; Draeger, A. ; Djonov, V.: Epithelial Transformations in the Establishment of the Blood–Gas Barrier in the Developing Chick Embryo Lung. In: *Developmental Dynamics* 235:68–81 (2006)

[29] Makanya, A.N. ; Sparrow, M.P. ; Warui, C.N. ; Mwangi, D.K ; Burri, P.H.: Morphological analysis of the postnatally developing marsupial lung: the quokka wallaby. In: *Anat. Rec.* 262:253-265 (2001)

[30] Meinhardt, H.: Morphogenesis of lines and nets. In: *Differentiation* 6:117-123 (1976)

[31] Menshykau, Denis ; Blanc, Pierre ; Unal, Erkan ; Sapin, Vincent ; Iber, Dagmar: An interplay of geometry and signaling enables robust lung branching morphogenesis. In: *Development* 141:1-11 (2014)

[32] Morrisey, Edward E. ; Hogan, Brigid L.: Preparing for the First Breath: Genetic and Cellular Mechanisms in Lung Development. In: *Developmental Cell Review* (2010)

[33] Petersen TH1, E.A. C. ; Zhao, L. ; Lee, E.J. ; Gui, L. ; Raredon, M.B. ; Gavrilov, K. ; Yi, T. ; Zhuang, Z.W. ; Breuer, C. ; Herzog, E. ; Niklason, L.E.: Tissue-engineered lungs for in vivo implantation. In: *Science* 329(5991):538-41 (2010)

[34] Powell, Frank L. ; Hopkins, Susan R.: Comparative Physiology of Lung Complexity: Implications for Gas Exchange. In: *Physiology* 19:55-60 (2004)

[35] Satelli, Arun ; Li, Shulin: Vimentin as a potential molecular target in cancer therapy Or Vimentin, an overview and its potential as a molecular target for cancer therapy. In: *Cell Mol Life Sci* 68(18): 3033–3046 (2011)

[36] Savagner, P. ; Yamada, K.M. ; Thiery, J.P.: The zinc-finger protein Slug causes desmosome dissociation, an initial and necessary step for growth factor-induced epithelial-mesenchymal transition. In: *J. Cell. Biol.* 137:1403-1419 (1997)

[37] Schachner, Emma R. ; Cieri, Robert L. ; Butler, James P. ; Farmer, C.G.: Unidirectional pulmonary airflow patterns in the savannah monitor lizard. In: *Nature* 506(7488):367-70 (2014)

[38] Schachner, Emma R. ; Hutchinson, John R. ; Farmer, C.G.: Pulmonary anatomy in the Nile crocodile and the evolution of unidirectional airflow in Archosauria. In: *PeerJ* 1:e60 (2013)

[39] S.H., Lee ; Shen, G.N. ; Jung, Y.S. ; Lee, S.J. ; Chung, J.Y. ; Kim, H.S. ; Xu, Y. ; Choi, Y. ; Lee, J.W. ; Ha, N.C. ; Song, G.Y. ; Park, B.J.: Antitumor effect of novel small chemical inhibitors of Snail-p53 binding in K-Ras-mutated cancer cells. In: *Oncogene* 29(32):4576-87 (2010)

[40] Shamir, Eliah R. ; Ewald, Andrew J.: Three-dimensional organotypic culture: experimental models of mammalian biology and disease. In: *Nat. Rev. Mol. Cell Biol.* 15(10):647-64 (2014)

[41] S.P., Wang ; Wang, W.L. ; Chang, Y.L. ; Wu, C.T. ; Chao, Y.C. ; Kao, S.H. ; Yuan, A. ; Lin, C.W. ; Yang, S.C. ; Chan, W.K. ; Li, K.C. ; Hong, T.M. ; Yang, P.C.: p53 controls cancer cell invasion by inducing the MDM2-mediated degradation of Slug. In: *Nat. Cell. Biol.* 11(6):694-704 (2009)

[42] Spurlin, James I. ; Lwigale, Peter: A technique to increase accessibility to late-stage chick embryos for in ovo manipulations. In: *Dev. Dyn.* 242(2):148-54 (2013)

[43] Tanaka-Matakatsu, Miho ; Uemura, Tadashi ; Oda, Hiroki ; Takeichi, Masatoshi ; ; Hayashi, Shigeo: Cadherin-mediated cell adhesion and cell motility in Drosophila trachea regulated by the transcription factor Escargot. In: *Development* 122:3697-3705 (1996)

[44] Turing, Alan M.: The Chemical Basis of Morphogenesis. In: *Bull Math Biol.* 52(1-2):153-97 (1990)

[45] Varner, Victor D. ; Nelson, Celeste M.: Cellular and physical mechanisms of branching morphogenesis. In: *Development* 141:2750-2759 (2014)

[46] Ward, H.E. ; Nicholas, T.E.: Alveolar type I and type II cells. In: *Aust N. Z. J. Med.* 14(5 Suppl 3):731-4 (1984)

[47] WHO: Chronic obstructive pulmonary disease (COPD). In: *http://www.who.int/mediacentre/factsheets/fs315/en/* (2015)